Original scientific paper

A generalized mathematical model to understand the capacity fading in lithium ion batteries
Effects of solvent and lithium transport

Abhishek Deshpande, Saksham Phul, Balaji Krishnamurthy[✉]

Department of Chemical Engineering, BITS Pilani, Hyderabad 500078, India

[✉]Corresponding Author: balaji.krishb1@gmail.com; Tel: +91-040-66303552; Fax:+91-040-66303998

Abstract

A general mathematical model to study capacity fading in lithium ion batteries is developed. The model assumes that the formation of the Solid Electrolyte Interphase (SEI) layer is the primary reason behind the capacity fading in lithium ion batteries. Previous models have assumed that either the solvent or the lithium plays a key role in the film formation reaction which drives the capacity fading in lithium ion batteries. The current model postulates that the solvent species and lithium ions could play a limiting role in the capacity fade in a lithium ion battery. The model studies the concentration profiles of the solvent species and lithium ions at the electrode/film interphase as a function of diffusion and migration parameters. Model predictions are found to fit experimental data very well.

Keywords

Kinetics; Solid electrolyte interphase; Diffusion; Migration

1. Introduction

Lithium ion batteries are currently the main focus of research in the field of battery technology. However, the main problems with the lithium ion battery technology remains the capacity fading which occurs in the battery. Several mathematical models [1-15] currently exist which study the capacity fading in lithium ion batteries. Most of these models assume that the formation of the Solid Electrolyte Interphase layer (SEI) on the anode during storage and the initial charging discharging cycles is the principal reason behind the capacity fading in lithium ion batteries. Some of these models [6-8,15] assume that the decomposition of the solvent is the principal reason behind the formation of the SEI layer. They assume that the solvent species controls the rate

determining step in the film formation reaction and the lithium ions do not play a major role in the process because they are in abundance. A few models [10] suggest that the transport of electrons and interstitials dominate the film formation process. Some models have tried to study capacity fading in lithium ion batteries as a function of film formation on the cathode of the battery [16,17]. However, none of the above existing models study the capacity fading in a lithium ion battery by trying to understand the transport of both the solvent species and lithium ions through the SEI layer on the anode. We have tried to understand this in the present model.

2. Model development

Figure 1 shows the schematic of the formation of the SEI layer. The solvent and lithium ions are assumed to move from the film/electrolyte interphase to the film/electrode interphase. The motion of the solvent species is only because of diffusion while the motion of the lithium ions is due to diffusion and migration (due to the potential drop across the SEI layer and the lithium ions being charged). The following reaction from Agubra [18] is proposed to be the principal reaction behind the formation of the SEI layer:

$$(CH_2O)_2CO(S) + 2e^- + 2Li^+ \rightarrow Li_2CO_3 + C_2H_4(g) \tag{a}$$

Here, ethylene carbonate is considered to be the solvent species and lithium carbonate is considered to be the product.
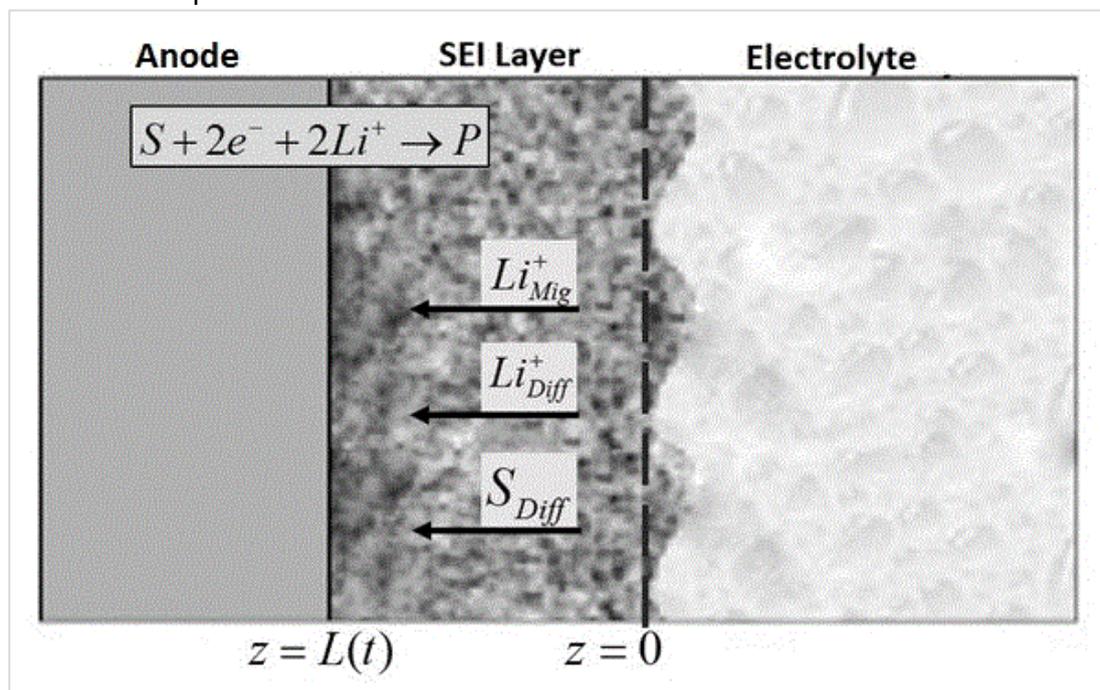
Figure 1. *Schematic showing the transport of lithium ions and solvent species in the SEI layer of a lithium ion battery.*

Model Assumptions

a) The SEI layer is considered to be homogenous in composition. It is considered to be a solid phase.

b) The growth of the SEI layer is considered to be a one dimensional phenomena on the anode. The SEI formation reaction is assumed to occur only at the electrode/film interphase.

c) The SEI layer is assumed to comprise only of Li_2CO_3 formed as a result of the reaction between ethylene carbonate/dimethyl carbonate with the lithium ions. $LiPF_6$ is assumed to be the salt used in the reaction.

d) The capacity fading in the battery is assumed to be solely because of the formation of the SEI layer on the anode of a lithium ion battery.

e) The model assumes that both the concentration of lithium ions and solvent ions at the electrode/film interphase play a role in the film formation reaction. The lithium ions are assumed to move from the film/electrolyte interphase to the electrode/film interphase by diffusion and migration while the solvent ions are assumed to move from the film/electrolyte interphase to the electrode/film interphase only by diffusion (since the solvent species are not charged).

f) The effects of film dissolution and acid attack on the film is considered to be negligible. The SEI formation reaction is considered to proceed with a second order rate constant k (since both the lithium and solvent species play a key role).

g) The model assumes that the formation of the SEI layer on the anode is the principal reason for capacity fading in lithium ion batteries. The capacity losses as a result of film formation on the cathode is assumed to be negligible.

h) The model assumes that the electrode/film interphase is the moving boundary and the film/electrolyte interphase remains stationary.

i) The value of the potential at the electrode/film interphase is assumed to zero. This in essence means that the model assumes that while the potential drop across the SEI layer is a major factor in the transport of lithium ions, it does not play a major role in the reaction at the electrode/film interphase. The potential drop across the SEI layer is assumed not to vary with time and decreases linearly from the film/electrolyte interphase to the electrode/film interphase. We follow our earlier work [19] and assume that the diffusivity and mobility of lithium ions are related by the Nernst Einstein equation.

j) In accordance with the model of Battaglia and Newman [20], the model assumes that an initial film thickness for computational purposes. The concentrations of the solvent species and lithium ions are assumed to a constant across the very thin film at initial time.

k) The concentration change in the electrolyte as a result of solvent consumption in the SEI layer is considered to be negligible.

3. Transport Equations

The differential mass balance for a material species k in a film phase is given by

$$\frac{\partial C_k}{\partial t} = -\nabla N_k + R_k \tag{1}$$

Dilute solution theory specifies the mass flux N_i as

$$N_i = -Z_k u_k F C_k \nabla C_k - D_k \nabla C_k + C_k v \tag{2}$$

as the sum of the migration, diffusion and convective contributions. Since the convective contribution is zero for both lithium ions and solvent molecules in this system, the transport equations for the solvent molecules in this particular system can be written as (assuming that the homogenous reaction in the film is zero)

$$\frac{\partial C_s}{\partial t} = D_s \frac{\partial^2 C_s}{\partial z^2} \tag{3}$$

since the only mode of transport of solvent molecules is through diffusion. From equation (2) and relating the diffusivity of lithium ions with the mobility by Nernst Einstein's equation [19], we can write the following equation to define the flux of lithium ions

$$N_i = -D_i \left(z_i C_i \frac{\Delta v^*}{l} + \frac{\partial C_i}{\partial z} \right) \tag{4}$$

where Δv^* refers to the dimensionless potential drop across the SEI layer and l refers to the thickness of the SEI layer at any given time.

Inserting equation (4) into (1), gives us the governing equation for the transport and material balance of lithium ions (assuming that the homogenous reaction within the film is zero and the transport by convection is also zero)

$$\frac{\partial C_{Li}}{\partial t} = -D_{Li} \frac{\partial^2 C_{Li}}{\partial z^2} + y D_{Li} \frac{\Delta v^*}{l} \frac{\partial C_{Li}}{\partial z} \tag{5}$$

Δv^* refers to the dimensionless potential drop across the SEI layer. The stoichiometric relation between the consumption of solvent molecules and lithium ions is taken into account in formulating these equations. The boundary conditions for solving equations (3) and (5) are given as follows:

At the film/electrolyte interphase ($z = 0$), the initial concentration of C_s is assumed to be C_o mol/m^3 which is a defined and known concentration. The initial concentration of lithium at the film/electrolyte interphase at $z = 0$ is also assumed to be the same as the solvent concentration and hence is taken as C_o mol/m^3. At the electrode/film interphase ($z=l(t)$), the boundary conditions are defined by the rates of reactions for the particular species. Thus the boundary conditions can be defined as

At $z = 0$ $C_S = C_0$ mol/m^3 (for all t) $\tag{6}$

At $z = 0$ $C_{Li} = C_0$ mol/m^3 (for all t) $\tag{7}$

At $z = l(t)$ $AD_S \frac{\partial C_S}{\partial z} = -(kC_{Li}C_S)V_l$ $\tag{8}$

At $z = l(t)$ $AD_{Li} \frac{\partial C_{Li}}{\partial z} = -(2kC_{Li}C_S)V_l$ $\tag{9}$

At $t = 0$ $D_s = C_{Li} = C_0$ (for all z) $\tag{10}$

where A is the cross sectional area of the reaction zone(for the formation of the SEI layer) and V_l is the volume of the reaction zone. Equations 8 and 9 equate the diffusive fluxes at the interphases with the reaction rate of the film formation.

Equations 3, 5, 6, 7, 8, 9 and 10 can be written in the following dimensionless forms for the concentration profiles of the solvent molecules and lithium ions.

$$\frac{\partial C_{So}}{\partial t^*} = -D_2 \frac{\partial^2 C_{So}}{\partial z^{*2}} \tag{11}$$

$$\frac{\partial C_{Lio}}{\partial t^*} = D_1 \frac{\partial^2 C_{Lio}}{\partial z^{*2}} + y D_1 \Delta v^* \frac{\partial C_{Lio}}{\partial z^*} \tag{12}$$

At $z^* = 0$ $C_{So} = C_{Li0} = 1$ (for all t^*) $\tag{13}$

At $z^* = 1$ $\left(D_2 \frac{\partial C_{So}}{\partial z^*} \right) = -C_{So} C_{Lio}$ $\tag{14}$

At $z^* = 1$ $\left(D_1 \frac{\partial C_{Lio}}{\partial z^*} \right) = -2C_{So} C_{Lio}$ $\tag{15}$

At $t^* = 0$ $\quad$ $C_{So} = C_{Li0} = 1$ (for all z^*) $\hfill$ (16)

The definition of the different variables and dimensionless groups are given in Tables 1 and 2. Equations 11-16, are the dimensionless equations and boundary conditions to be solved for evaluating the concentration profiles of the solvent and lithium species at the electrode/film interphase. Further the fractional capacity loss in the battery is given by the equation,

Dimensionless Fractional capacity loss = $(C_{Lioi} - C_{Liot})/C_{Lioi}$

where C_{Lioi} is the dimensionless initial concentration of lithium ions at the electrode/film interphase, C_{Liot} is the dimensionless concentration of lithium ions at the electrode/film interphase at any given time. By calculating the C_{Liot} value from the code, we are able to calculate the loss of lithium ions at any given time which relates to the lithium consumed in the reaction forming the SEI layer. Using the equation for fractional capacity loss, we find out the capacity loss in the battery.

Table 1. Characteristic quantities used for Dimensional analysis in the model

Dimensionless variable	Dimensional variable	Characteristic quantity
Z^*	Z	L - initial film thickness
C_{So}, C_{Lio}	C_S, C_{Li}	C_o - initial concentration of lithium at electrolyte/film interphase
Δv	Δv	RT/F
t^*	t	$1/kC_o$

Table 2. Interpretation of Dimensionless groups used in model

Dimensionless groups	Interpretation
$D_1 = D_{Li}/kC_o l^2$	The rate of diffusion coefficient of lithium to the rate constant of the SEI formation reaction.
$D_2 = D_s/kC_o l^2$	The ratio of diffusion coefficient of solvent species to the rate constant of the SEI formation reaction.
$\Delta v^* = F\Delta v/RT)$	Dimensionless voltage

4. Numerical solution

Equations 11 to 16 were solved numerically using MATLAB© with its predefined function called the 'pdepe solver' which solves initial-boundary value problems for systems of partial differential equations in one space variable z and time t. The pdepe solver converts the PDEs (Partial Differential Equations) to ODEs (Ordinary Differential Equations) using a second-order accurate spatial discretization based on a fixed set of user-specified nodes.

In this work, a set of equations consisting of two coupled partial differential equations with dependent boundary conditions which represent the solvent and lithium concentrations were solved for the concentration profiles at the electrode/film interphase using the pdepe solver. For the accuracy of solution, a fine mesh was created by dividing the film layer thickness into 100 spacesteps and similarly dividing the total time into 100 timesteps. This ensured uniformity in all the calculations. Equations 11-16 were solved using MATLAB for the defined geometry for the concentration profiles of the solvent and lithium ions.

5. Results and Discussion

Figure 2 shows the variation of dimensionless lithium concentration at the electrode/film interphase as a function of dimensionless time with varying values of D_1 and constant values of D_2.

Since the capacity loss of the battery is expressed in terms of lithium concentration, we have varied the value of D_1 and kept D_2 a constant. We wish to emphasize here that D_1 and D_2 are dependent on *l*, the characteristic length. However, we have assumed the characteristic length to be the initial value of film thickness used for computational purposes (0.1 nm). This essentially means that D_1 and D_2 do not vary with time. The potential drop across the SEI layer is kept at 0.0 V for this simulation (this in effect means that the lithium ions are driven only by diffusion and not by migration). D_1 is varied to find the effect of the diffusivity of lithium ions on the concentration of the lithium ions at the electrode/film interphase and the reaction at the interphase. Simulations are run for 3 different values of D_1. Assuming that the values of the reaction constant k is kept constant and C_o is constant, this means that the only parameters which is varying is the diffusion coefficient of lithium. Literature postulates that the diffusion coefficient of lithium through crystalline solids varies anywhere between 10^{-7} cm^2/s to 10^{-15} cm^2/s [21,22]. Figure 2 shows that with increasing values of the diffusivity of the lithium ions, there is a defined change in the concentration of lithium ions at the electrode/film interphase. The higher the value of the diffusion coefficient of lithium ions, the higher the concentration of lithium ions at the electrode/film interphase.
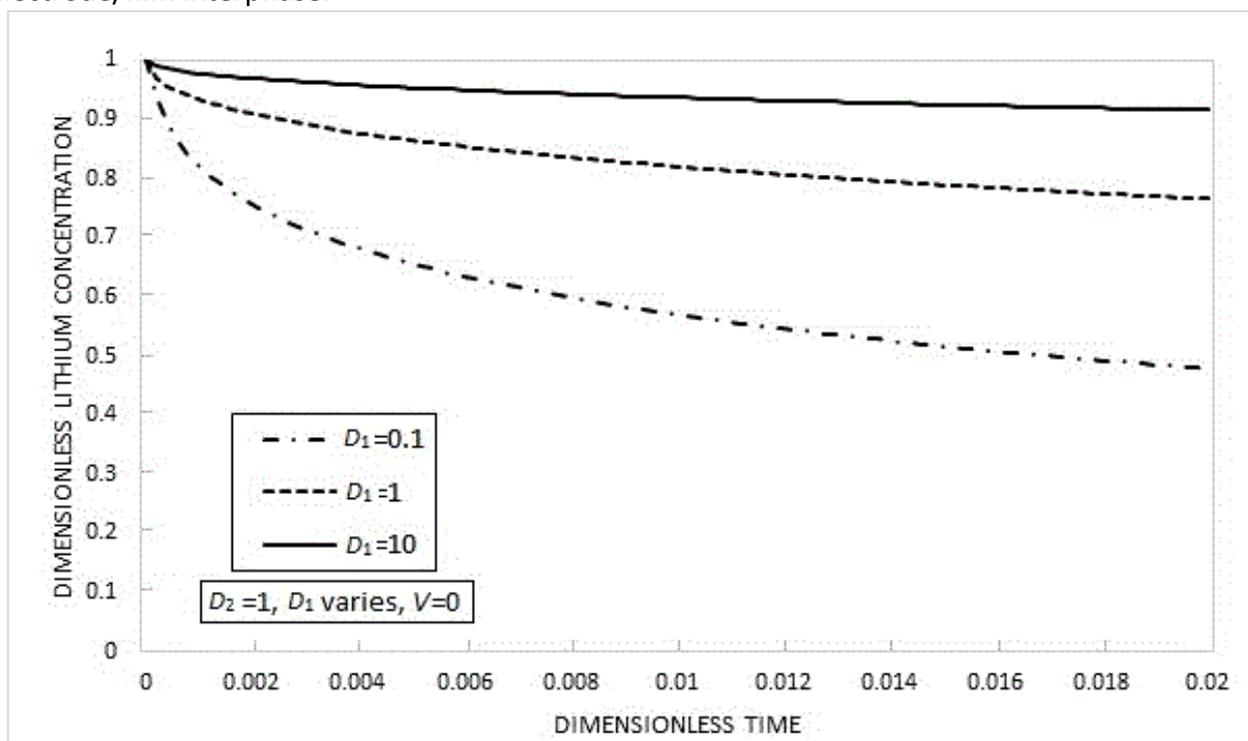
Figure 2. *Variation of dimensionless lithium ions at the electrode/film interphase as a function of varying* D_1 *values.* D_2 *= 1 and potential drop across the SEI layer is 0.*

This indicates that though increasing diffusivity of the lithium ions increases the reaction rate at the electrode/film interphase, there is an increase in the accumulation of lithium ions at the electrode/film interphase which is reflected in the results. Figure 3 shows the concentration profile of the solvent species for varying values of D_1 and a constant value of D_2. With higher values of D_1, the reaction rate of the lithium ions at the electrode/film interphase increases. This results in additional consumption of lithium ions and solvent molecules. However, with D_2 being maintained constant, the diffusion coefficient of solvent molecules remains a constant leading to a constant flux of solvent molecules to the electrode/film interphase. This leads to decreasing values of the solvent concentration at the electrode/film interphase with increasing values of D_1.
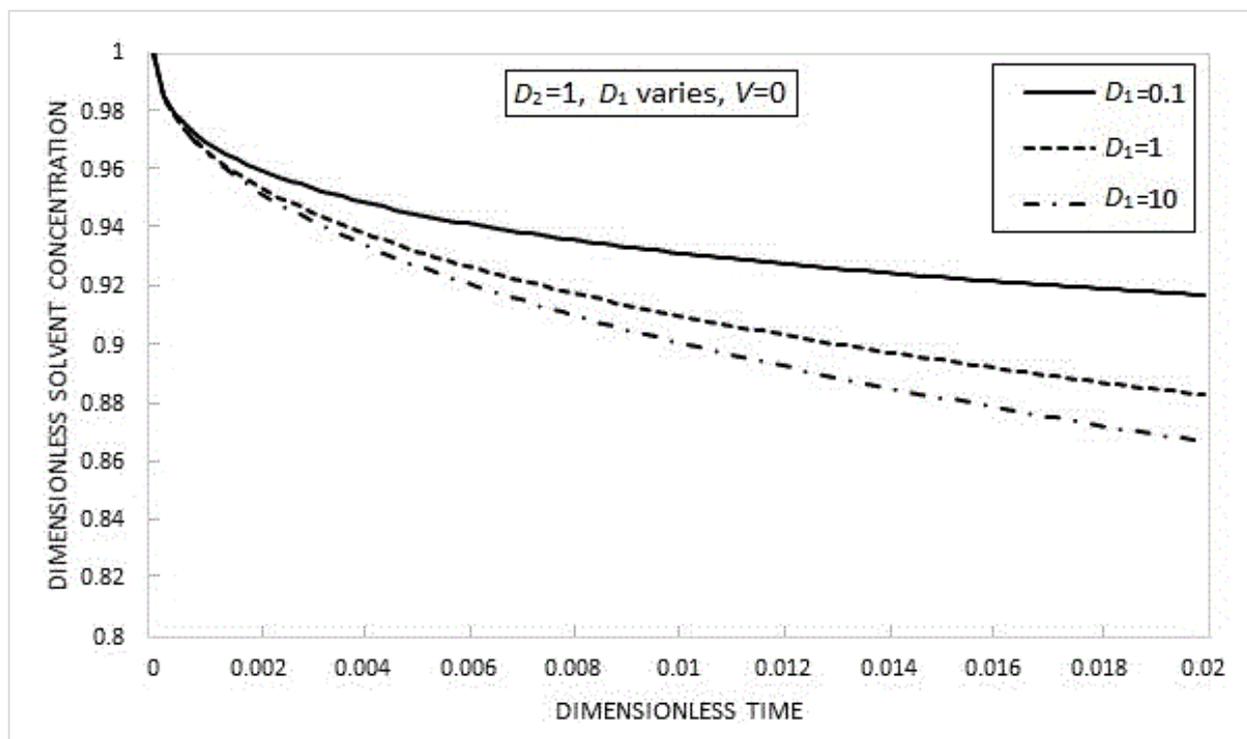
Figure 3. *Variation of dimensionless solvent concentration at the electrode/film interphase as a function of varying* D_1 *values.* $D_2 = 1$ *and* $V = 0$.

Figure 4 shows the variation of dimensionless concentration of lithium ions at the electrode/film interphase as a function of varying values of D_1 and constant value of D_2, but with a potential drop of 0.2 V applied across the SEI layer. While the concentration profiles are found to follow a similar pattern as Figure 2, it is seen that the consumption of lithium ions is more when the potential drop is applied across the SEI layer. The potential drop seems to be increasing the transport of lithium ions from the film/electrolyte interphase to the electrode/film interphase through migration effects. This increases the reaction rate for the SEI film formation which in turn increases the consumption of lithium ions at the interphase. A comparison of Figure 2 with Figure 4 for constant values of D_1 indicates this. To further study the effect of potential drop across the SEI layer on the film formation process, we study the concentration of lithium ions at the electrode/film interphase for three different values of voltages 0.0, 0.1 and 0.2 for constant values of D_1 and D_2. Figure 5 shows this graph. The dimensionless lithium concentration is seen to change with changing values of applied potential across the SEI layer. It is seen that potential drops across the SEI layer ranging from 0.1 to 0.2 V causes additional consumption of lithium ions at the interphase. This in essence is because of the additional transport of lithium ions from the film/electrolyte interphase to the electrode/film interphase caused by the migration effect due to the potential drop across the SEI layer. We wish to indicate that very little experimental data exists in literature which actually studies the potential drop across the SEI layer. Since the SEI film thickness used in our experimental fits are of the order of 10 -300 nm, we have used a maximum potential drop of 0.2 V across the SEI layer. However, while several experimentalists have looked at the onset potential for the formation of the SEI layer, no data exists which actually measures the potential drop across the SEI layer.
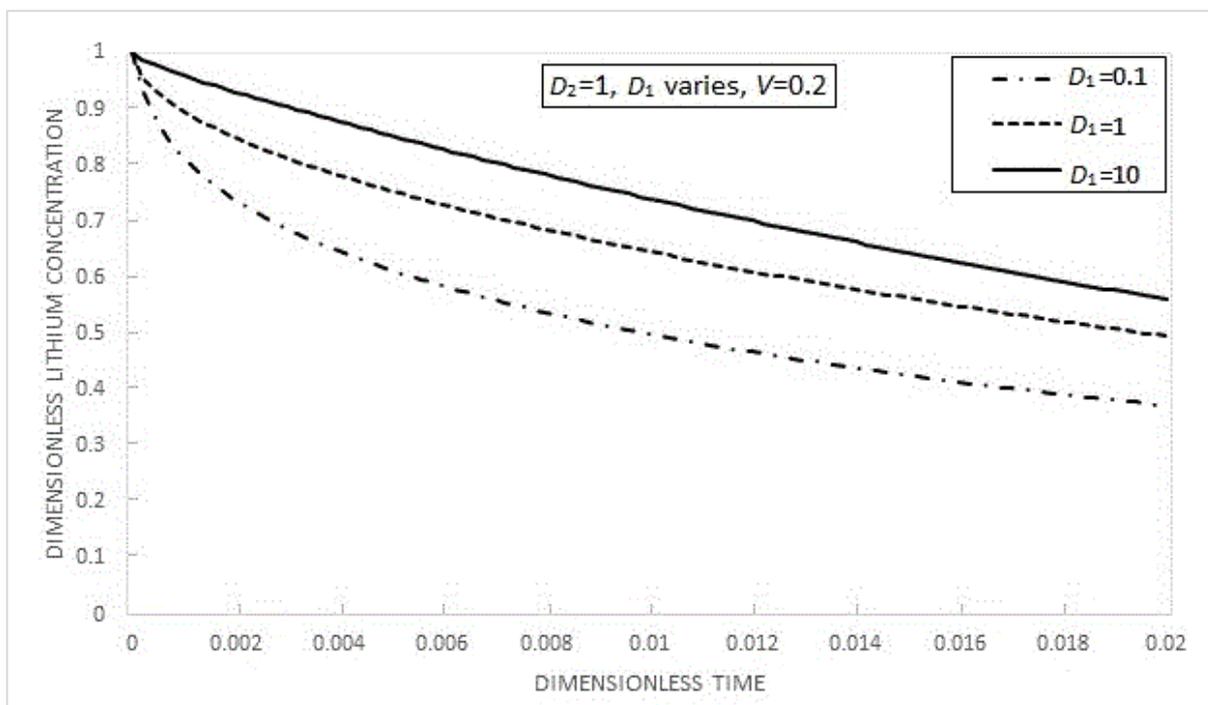
Figure 4. *Graph showing the variation of dimensionless lithium concentration at the electrode/film interphase as a function of varying D_1 values. D_2 = 1 and V = 0.2.*
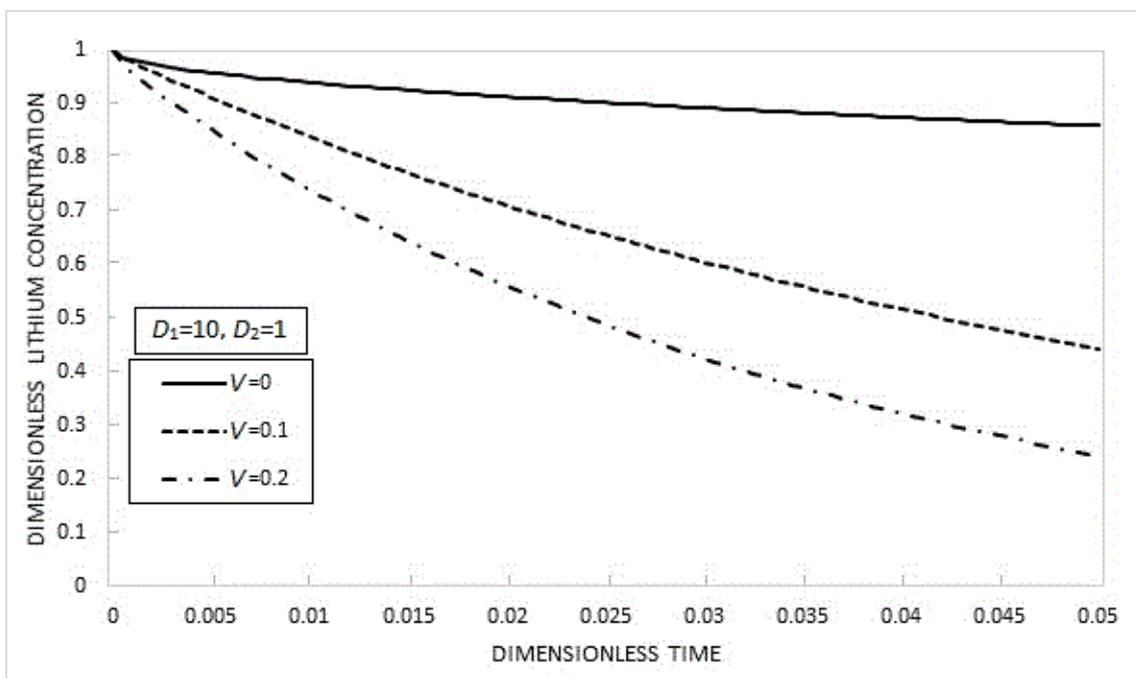
Figure 5. *Effect of potential drop across the SEI layer on the concentration of lithium ions at the electrode/film interphase.*

Figure 6 shows the concentration of the solvent species at the electrode/film interphase at constant value of D_1 and varying values of D_2, at $V = 0$. Comparing Figure 6 and Figure 7 (solvent concentration at the electrode/film interphase for $V = 0.2$) it is seen that there is very little difference in the solvent concentration as a result of the potential drop across the SEI layer. This shows that while the potential drop across the SEI layer plays a major role in the transport of lithium ions, it plays very little role in the transport of solvent species across the SEI layer. However, the increase in the reaction rate of lithium ions caused by the potential drop across the SEI layer can cause additional consumption of the solvent species.
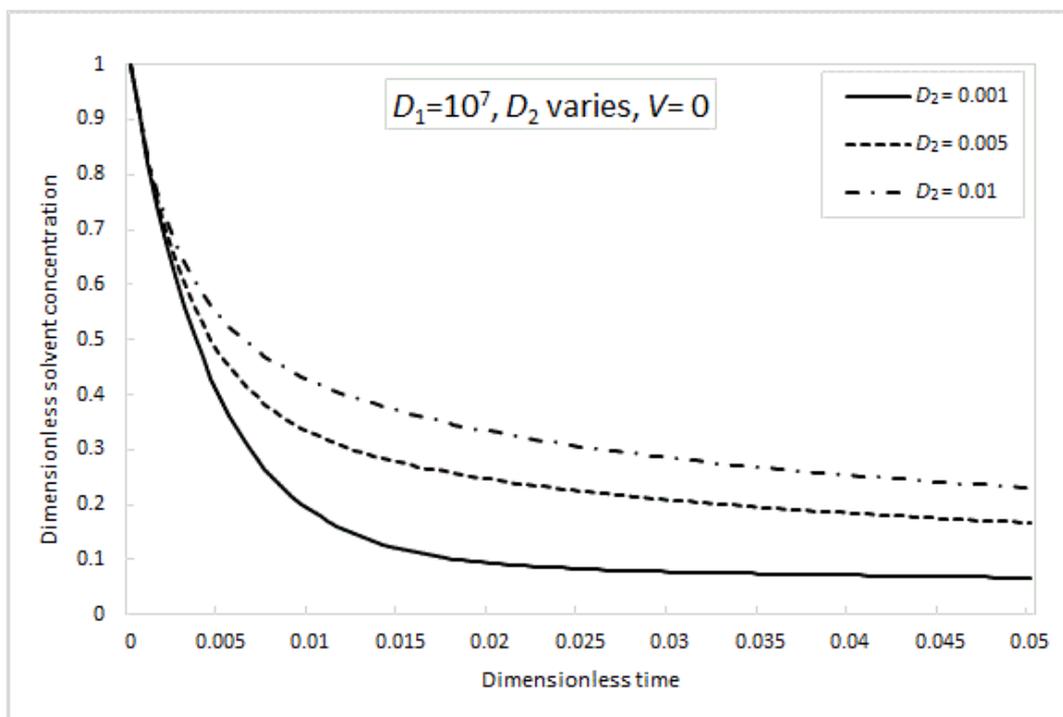
Figure 6. *Variation of dimensionless solvent species at the electrode/film interphase with varying* D_2 *values, V = 0.0.*
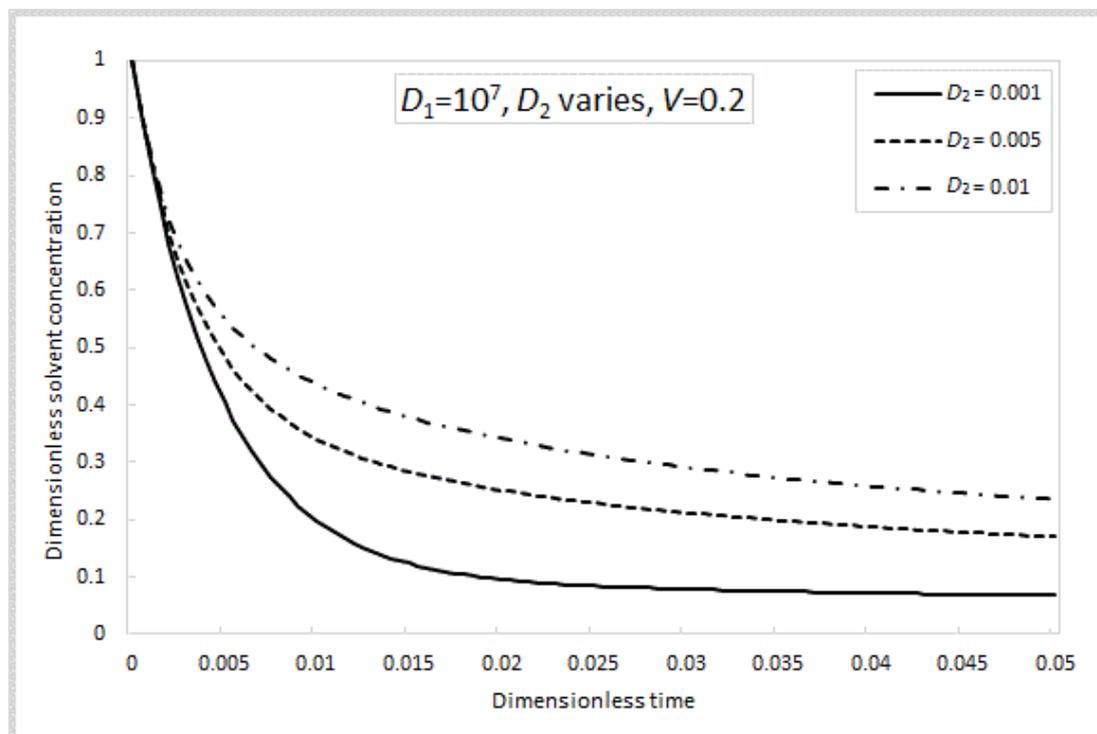
Figure 7. *Variation of dimensionless solvent species at the electrode/film interphase with varying* D_2 *values, V = 0.2.*

Figure 8 shows the comparison of modeling results for capacity fade with experimental data for the HE [12] type cells. . Since the capacity fade is directly related to the fraction of lithium ions, we have kept D_2 constant for these simulations (10^5). The potential drop across the SEI layer for these simulations is kept at 0.2 V. The values of D_1 are varied to fit modeling results with experimental data. It is seen that higher capacity fade is seen at lower values of D_1. Thickness of the SEI layer can

be found from capacity loss curves with the equation given in our earlier work [6]. Table 3 shows the list of parameters used for fitting simulation results with experimental data.
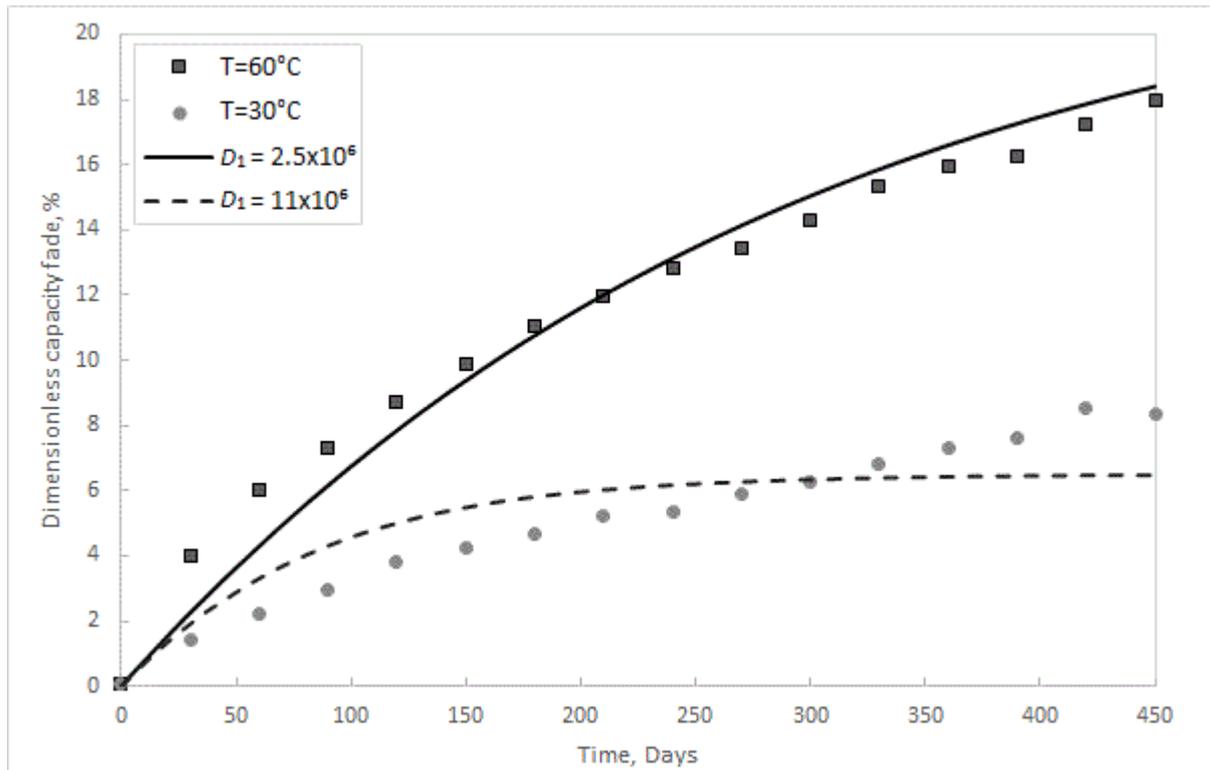
Figure 8. *Simulation fit with experimental data for HE type cells [12]*

Table 3. *Parameters used for fitting simulation results with experimental data*

Parameters	Range of values
C_o	10^3 - 10^5 mol/m^3
k	10^{-7} m^3/mol s - 10^{-14} m^3/mol s
l	0.1 nm
D_{Li}	10^{-12} m^2/s - 10^{-22} m^2/s
D_s	10^{-19} m^2/s - 10^{-28} m^2/s

Figure 9 shows the comparison of modeling results with experimental data for the MP type cells [12]. Simulation results are run at four different temperatures-15, 30, 45 and 60 °C. D_2 values are maintained a constant at 10^5 for these simulations. While modeling results are seen to fit very well with experimental data, it is seen that the highest capacity fading is seen at the lowest values of D_1. Since $D_1 = D_{Li}/kC_o l^2$) and since the values of C_o and l remain a constant, the only varying parameters with temperature are D_{Li} and k. The diffusion coefficient of lithium ions is seen to vary with temperature according to the Eyring's equation $D = D_o e^{-Ed/RT}$ and the rate constant is seen to vary with temperature according to the Arrhenius equation $K = A_o e^{-Ea/RT}$. Hence, both Figures 8 and 9 indicate that highest capacity fade is seen at higher values of the rate constant indicating that the rate of increase of the rate constant k with temperature is much higher than the rate of increase of diffusion coefficient with temperature. This in turn indicates that the activation energy barrier for the kinetic reaction is lower than the diffusion process implying that the kinetics of the film formation reaction is a much faster process than the diffusion. The results confirm the observations from previous researchers [15].
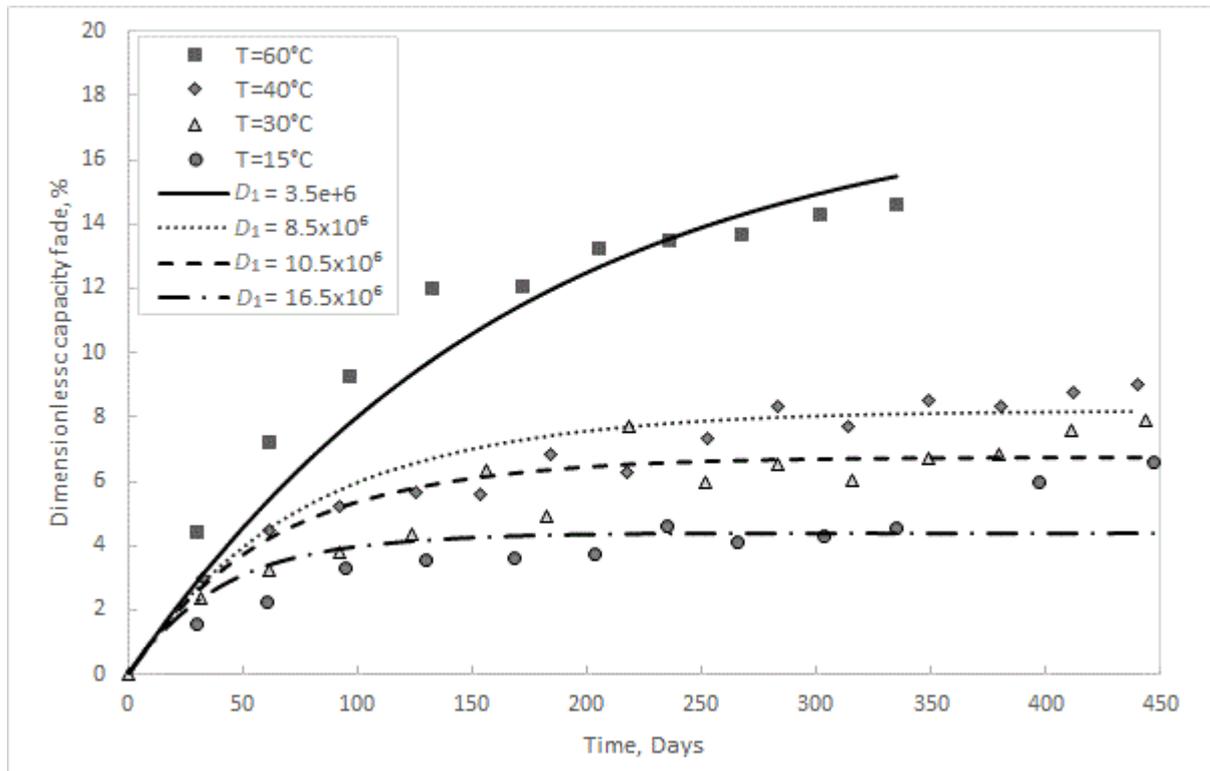
Figure 9. *Simulation fit with experimental data for MP type cells* [12]

Figure 10 and 11 shows the comparison of modeling results with experimental data for cells studied by Grolleu *et al.* [23] and Prada *et al.* [24]. As seen previously, modeling results are seen to fit very well with experimental data. Figures 12,13 and 14 show the comparison of modeling results with experimental data from SAFT DD[25], Yardney cells [25] and Boryann Liaw *et al.* [26]. Modeling fits yield the same results-the activation energy barrier for the kinetic rate constant is much lower than that of the diffusion coefficient.
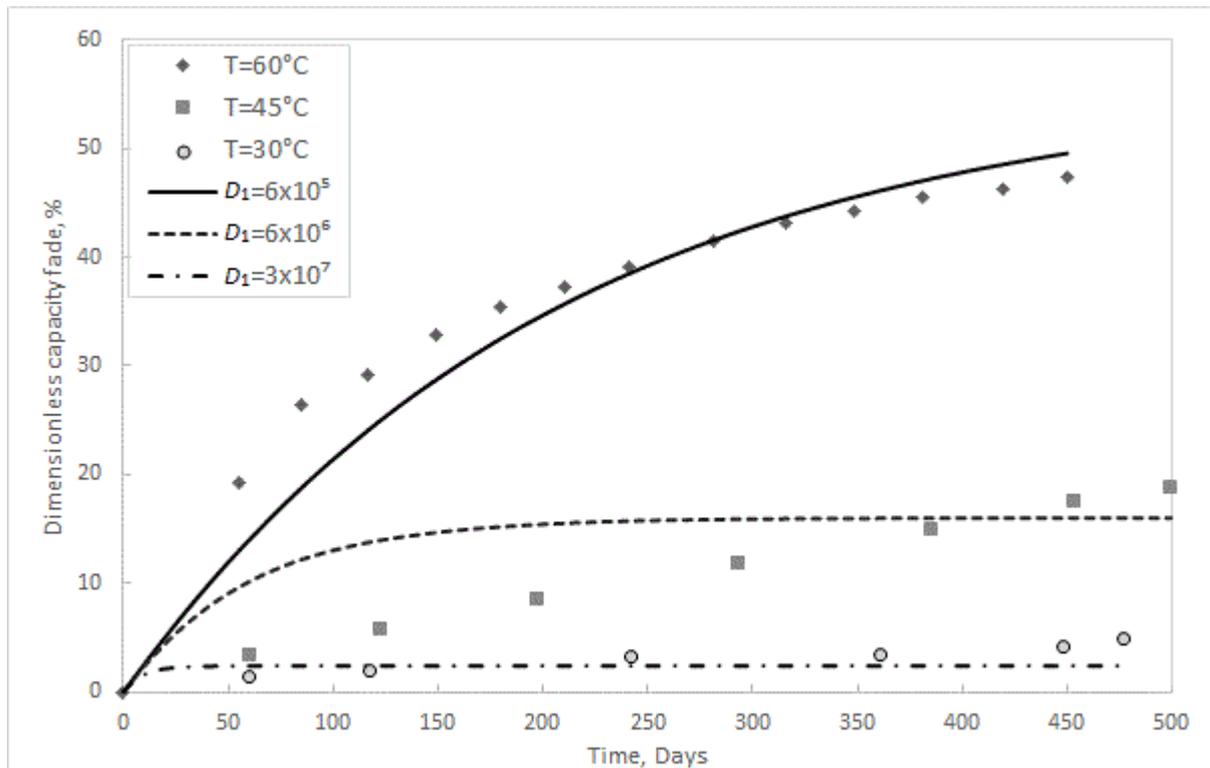
Figure 10. *Graph showing mModeling comparison with experimental data obtained from Grolleu* et al. [23].
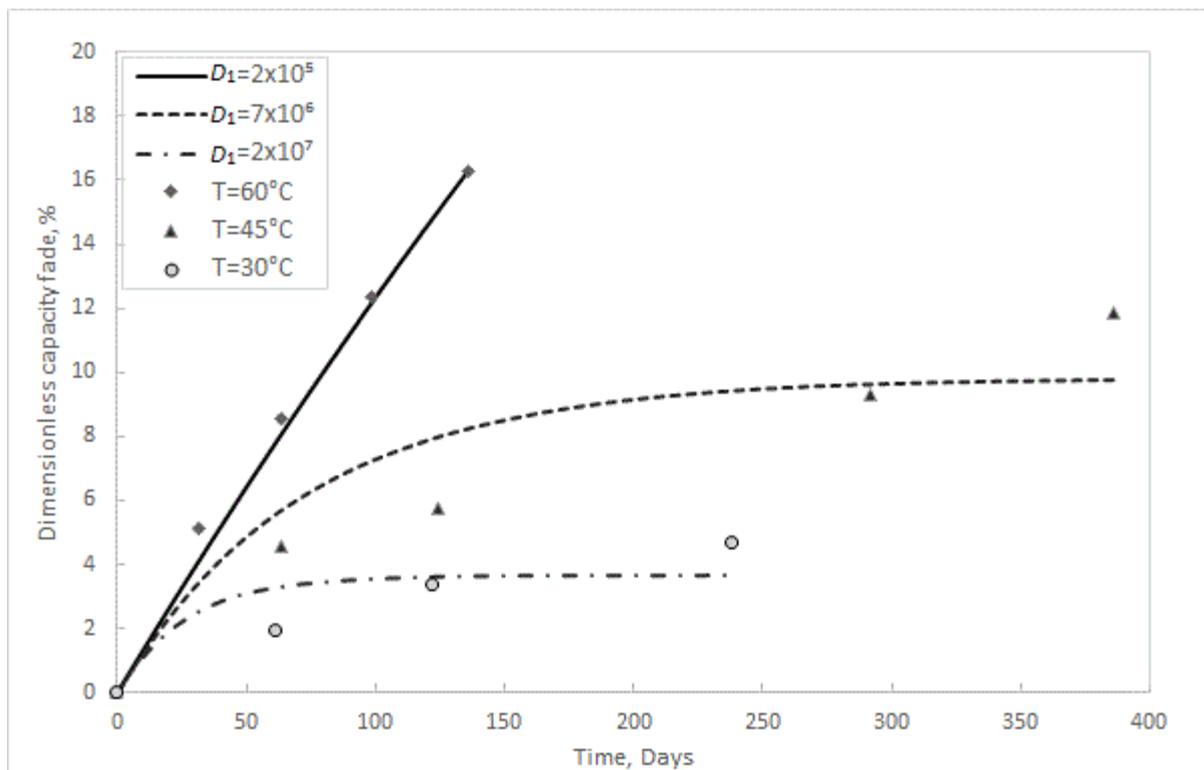
Figure 11. *Modeling comparison with experimental data obtained from Prada et al.* [24].
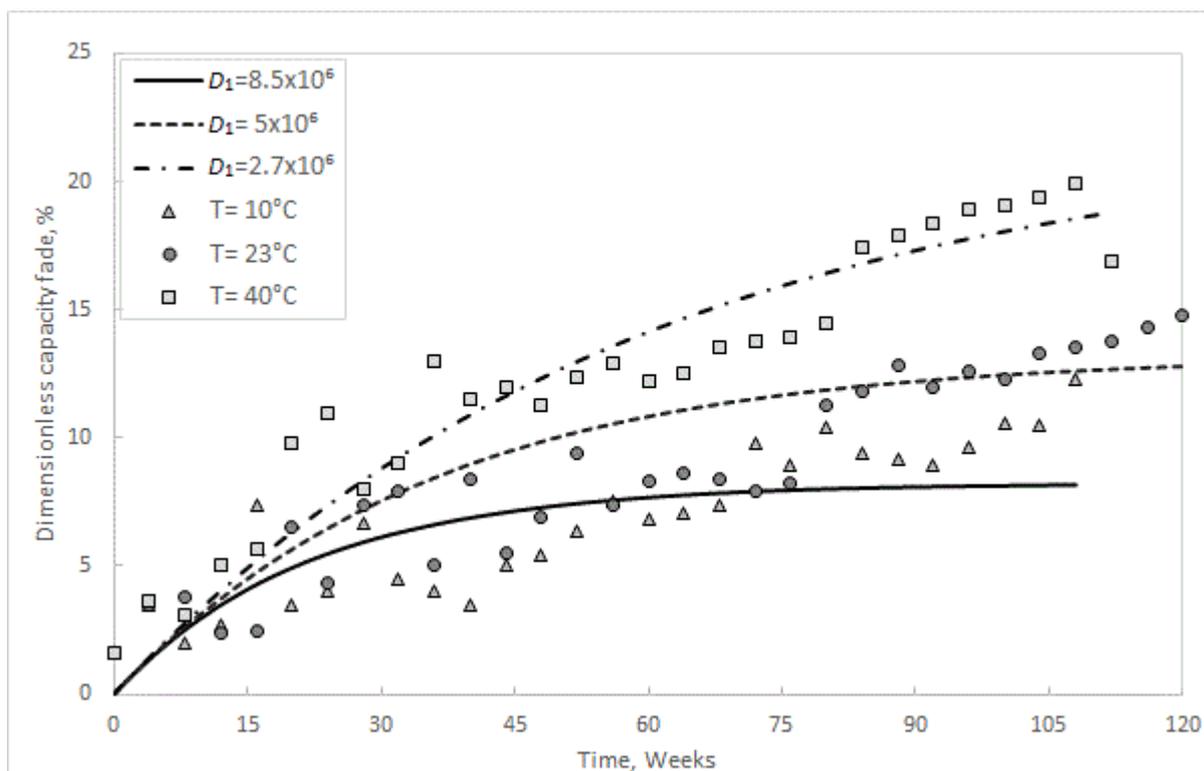
Figure 12. *Modeling comparison with experimental data obtained from SAFT DD^{25} cells.*
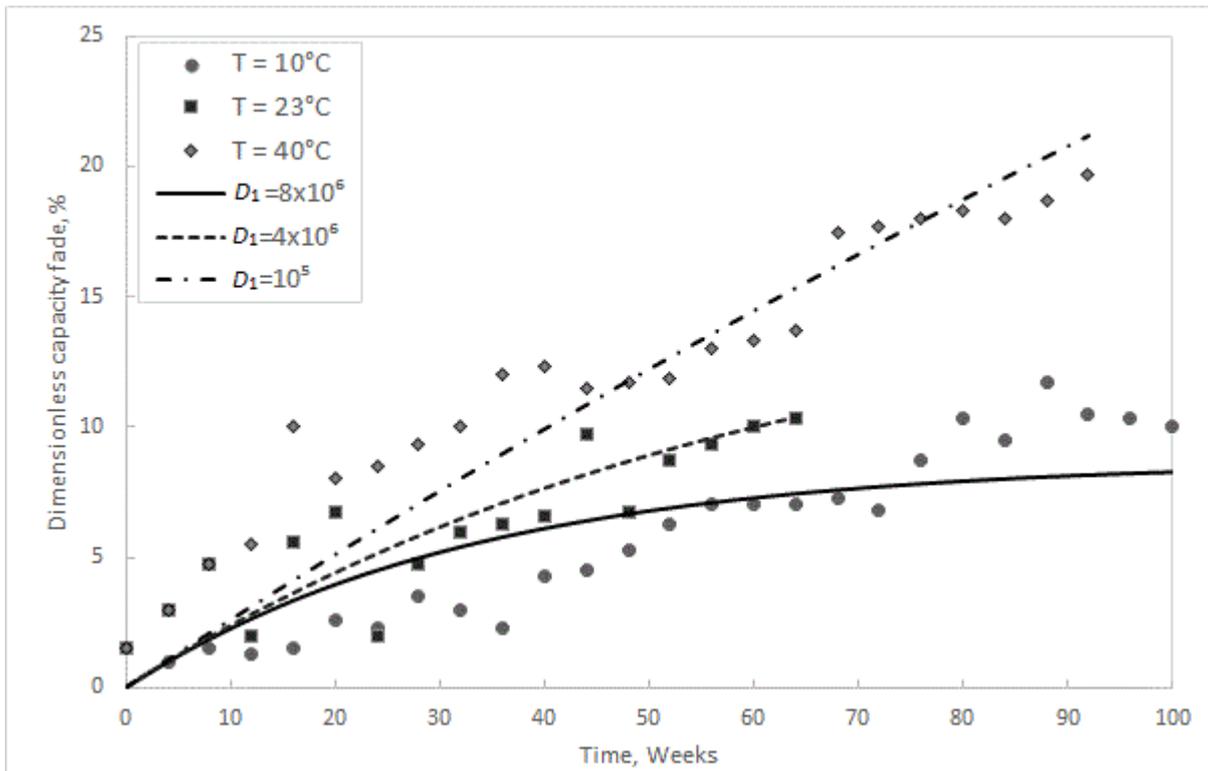
Figure 13. *Modeling comparison with experimental data obtained from Yardney type cells*[25]
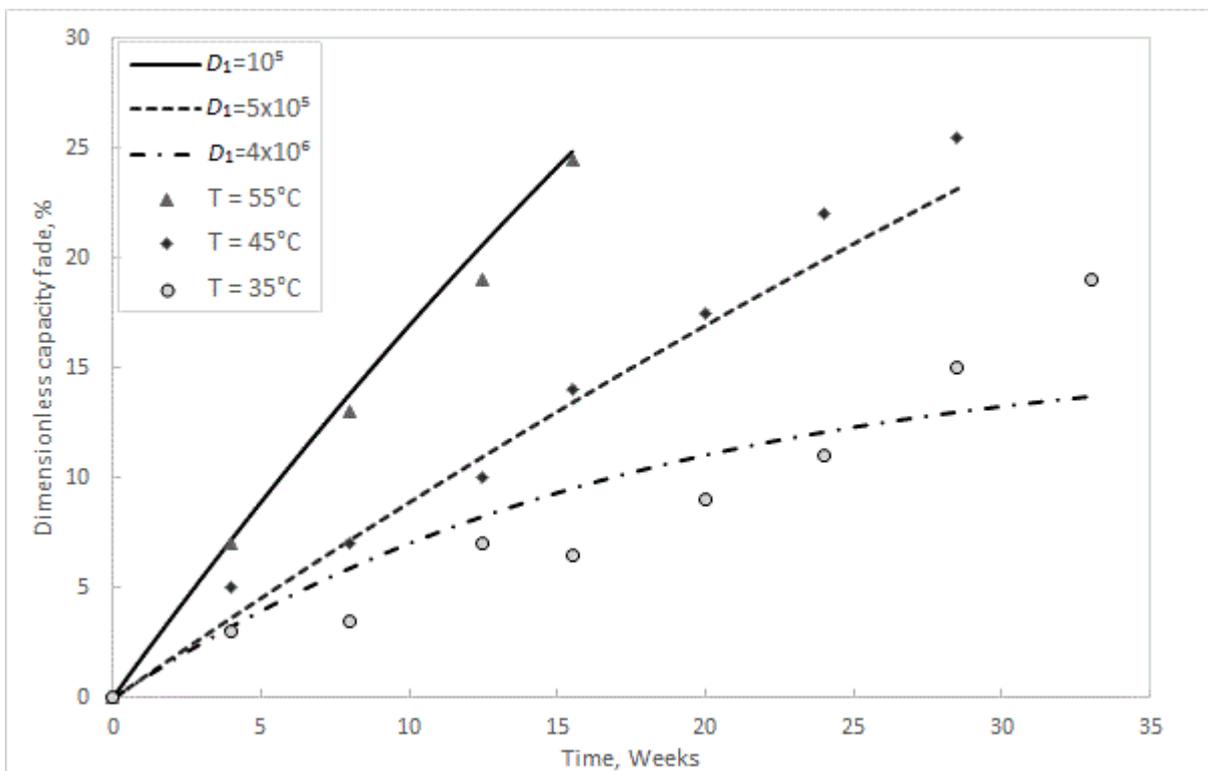
Figure 14. *Modeling comparison with experimental data obtained from Boryann* et al. [26]

6. Conclusions

A mathematical model is developed to study the capacity fading in lithium ion batteries. Unlike previous models, the model assumes that the capacity fading in lithium ion batteries is a function of solvent and lithium transport. Transport equations are developed to understand the concentration profiles of lithium ions and solvent species at the electrode/film interphase. Model results

indicate that while the diffusion coefficient of lithium ions and the diffusion coefficient of solvent species play a role in enhancing the film formation reaction at the electrode/film interphase, the potential drop across the SEI layer significantly enhances the transport of lithium ions across the SEI layer and hence the reaction rate at the electrode/film interphase. However, the potential drop across the SEI layer is not seen to affect the transport of solvent species across the SEI layer. Model results are found to predicate experimental data very well. Future work would include studying the effects of the potential drop on the reaction rate at the electrode/film interphase.

List of Symbols

N_i Flux of species, $m^2 s^{-1}$

F Charge on 1 mole of electron Coulombs

$\nabla\emptyset$ Potential gradient, $V m^{-1}$

D_i Diffusivity of species I, $m^2 s^{-1}$

D_{Li} Diffusion coefficient of lithium ions, $m^2 s^{-1}$

D_s Diffusion coefficient of solvent ions, $m^2 s^{-1}$

z Distance across the SEI film, m

z_i Valence of species, i

u_i ionic mobility of species i, $m^2 V^{-1} s^{-1}$

C_i Concentration of the species, $mol\ m^{-3}$

v Convective velocity of species, $m s^{-1}$

Δv Potential drop across SEI layer (this is also represented by V in the graphs), V

l SEI layer thickness, nm

t Time, s

y Stoichiometric coefficient

k Second order rate constant of the reaction, $L\ mol^{-1} s^{-1}$

C_o Dimensional initial concentration of lithium ions, $mol\ m^{-3}$

C_{Li} Dimensional concentration of lithium ions, $mol\ m^{-3}$

C_s Dimensional concentration of solvent species, $mol\ m^{-3}$

C_{Lio} Dimensionless concentration of lithium ions

C_{so} Dimensionless concentration of solvent species

$t*$ Dimensionless time

$z*$ Dimensionless distance between electrodes

A Cross section area of the electrode/film interphase where film formation happens, m^2

V_l Volume of the electrode/interphase region where film formation happens, m^3

References:

[1]   Y. S. Wang, J. T. Lee, *Electrochim. Acta* **142** (2014) 34-42.

[2]   R. Spotnitz, *J. Power Sources* **113** (2003)72-79.

[3]   L. Liu, J. Park, X. Lin, A. M. Sastry, and W. Lu, *J. Power Sources*.**268** (2014) 482-489.

[4]   R. Darling, J. Newman, *J. Electrochem. Soc.* **145** (1998) 990-996.

[5]   R. P. Ramasamy, J. W. Lee, B. N. Popov, *J. Power Sources* **166** (2007) 266 -272.

[6]   S. Shankarsubramanian, B. Krishnamurthy, *Electrochim. Acta* **70** (2012) 248-253..

[7]   H. J. Ploehn, P. Ramdass, R. E. White, *J. Electrochem. Soc.* **151** (2004) A256-A261.

[8]   M. Safari, M. Morcrette, C. Delacourt, *J. Electrochem. Soc.* **156** (2009) A145-A152.
[9]   J. Yan, G. Zhang, *Electrochim. Acta*. **53** (2008) 7069-7075.
[10]   J. Christensen, J. Newman, *J. Electrochem. Soc*. **151** (2004) A1977-A1985.
[11]   P. Ramadass, B. Haran, R. White, B. N. Popov, *J. Power Sources* **123** (2003) 230-237.
[12]   M. Broussely, S. Herreyre, R. J. Staniewicz, *J. Power Sources* **13** (2001) 97-104..
[13]   A. Coclasure, K. Smith, R. Kee, *Electrochim. Acta* **58** (2011) 33-39.
[14]   P. Ramadass, B. Haran, P. Gomadam, R. White, B. N.Popov, *J. Electrochem. Soc*. **151** (2004) A196-A202.
[15]   S. Ramesh, B. Krishnamurthy, *J. Electrochem.Soc*. **162** (2015) A545-A552.
[16]   Y. Dai, L. Cai, R. White, *J. Electrochem. Soc*. **160** (2013) A182-A189.
[17]   L. Cai, Y. Dai, M. Nicholson, R. E. White, K. Jagannatha, G. Bhatia*, J. Power Sources* **221** (2013) 191-197.
[18]   V. Agubra, J. Fergus, *J. Power Sources* **268** (2014)153-162.
[19]   B. Krishnamurthy, R. E.Whit, H. J. Ploehn, *Electrochimica Acta* **46** (2001) 3387-3394.
[20]   V. Battaglia and J. Newman, *J. Electrochem. Soc*. **142** (1995) 1423-1432.
[21]   S. Yang, Q. Wei, *Electrochimica Acta* **66** (2012) 88 -94.
[22]   P. Yu, B. N. Popov, J. Ritte, R. E. White, *J. Electrochem. Soc.* **146** (1999) 8 -15.
[23]   S. Grolleu, A. Dellaile, H.Gualous, P. Gyan, R. Revel, J. Bernard, E. R. Iglesias, J. Peter*, J. Power Sources* **255** (2014) 450-458.
[24]   E. Prada, J. Barnard, F. Huet*, J. Electrochem. Soc*. **160** (2013) A 616-A 628.
[25]   B. V. Ratnakumar, M. C.Smar, L. D. Whitcanack, *ECS Trans*. **25(36)** (2010) 297-305.
[26]   B. Liaw, P. Roth, R. Jungst, D .Doughty, *J. Power Sources* **119** (2003) 874-882.